Int J Cardiovasc Imaging (2015) 31:1361–1368
DOI 10.1007/s10554-015-0694-y

ORIGINAL PAPER

Maternal cardiac remodeling and dysfunction in preeclampsia: a three-dimensional speckle-tracking echocardiography study

Juan Cong[1,2,3,4] · Tingpan Fan[1] · Xiaoqian Yang[2,3,4] · Jacson Shen[5] · Guomei Cheng[2,3,4] · Zhan Zhang[2,3,4]

Received: 27 March 2015 / Accepted: 11 June 2015 / Published online: 16 June 2015

Abstract Aims preeclampsia (PE) is a pregnancy complication that remains a main cause of maternal morbidity and mortality. The aims of this study were to investigate left ventricle (LV) performance in PE and to compare maternal cardiac function between early-onset preeclampsia (EP) and late-onset preeclampsia (LP) by novel three-dimensional (3D) speckle-tracking echocardiography (STE) parameters while considering LV loading and shape. Methods and Results Two-dimensional echocardiography and 3D STE were performed in 43 women with EP, 41 women with LP, and 81 normal pregnancies. Global longitudinal strain (GLS), global circumferential strain (GCS), global area strain (GAS), and global radial strain (GRS) were measured using 3D speckle-tracking software. There was eccentric hypertrophy and reduced LV ejection fraction (EF) in PE; meanwhile, GLS in EP and LP, GCS in LP, as well as GAS and GRS in EP significantly decreased in PE versus controls. All 3D strain indices were correlated with gestation age. Increased left atrial (LA) volume index was detected in PE. Higher LV mass index and lower 3D-derived strain value were present in women with EP compared to that in women with LP. Conclusion PE cases exhibited significant eccentric hypertrophy, ventricular dysfunction, and LA remodeling. Furthermore, myocardial deformation abnormalities preceded chamber dysfunction in this hypertensive disorder complicated pregnancy. Compared with LP, women with EP demonstrated more remarkable cardiac damage.

Keywords Preeclampsia · Strain · Three-dimension · Speckle-tracking · Echocardiography

✉ Zhan Zhang
zhangzhanmd27@126.com

[1] Department of Ultrasonic Diagnosis, The Third Affiliated Hospital of Zhengzhou University, Zhengzhou 450052, Henan Province, China

[2] Department of Obstetrics and Gynecology, The Third Affiliated Hospital of Zhengzhou University, Zhengzhou 450052, Henan Province, China

[3] Henan Provincial Engineering Research Center for Perinatal Medicine, The Third Affiliated Hospital of Zhengzhou University, Zhengzhou 450052, Henan Province, China

[4] Henan Translational Medicine Engineering Laboratory for Maternal and Children's Health, The Third Affiliated Hospital of Zhengzhou University, Zhengzhou 450052, Henan Province, China

[5] Department of Orthopaedics, Massachusetts General Hospital, Boston, MA 02114, USA

Introduction

Preeclampsia (PE) is a pregnancy complication affecting 5 to 7 % of pregnant patients [1], and remains a main cause of maternal morbidity and mortality [2] due to high risks of subsequent hypercoagulability, heart failure, and the damage to the kidney, liver, and brain. Autopsy data have demonstrated that, compared with deaths in pregnancy from other causes, there is a tenfold prevalence of myocardial contraction band necrosis in PE cases [3].

Previous studies on cardiac changes in PE mainly focused on left ventricular (LV) systolic function; however, the results have been contradictory. Furthermore, even less data exist about changes in myocardial and diastolic function in PE, which have been shown to precede impairment of contractile dysfunction in the evaluation of most cardiac diseases [4, 5].

PE is commonly subdivided into early-onset (EP) and late-onset (LP) preeclampsia. Growing evidence shows that

EP and LP have different etiologies and should be regarded as two different types of the disease [6]. Dissimilar hemodynamic states have also been reported between EP and LP [7]. However, it is not clear whether there are differences in terms of chamber and myocardial function.

Three-dimensional (3D) speckle-tracking echocardiography (STE) indices are able to reflect the morphological state of the heart, further our understanding of myocardial deformation, and are even sensitive in detecting subtle myocardial damage [8]. In this study, we aimed to perform a comprehensive analysis of LV morphological and functional changes in PE using 3D STE indices together with conventional echocardiographic parameters and sought to ascertain whether there are differences in cardiac chamber and myocardial function between EP and LP.

Methods

Singleton PE pregnancies without any preexisting medical conditions were recruited for this study. None of the patients received antihypertensive therapy at least 3 days preceding the study. The criteria of the International Society for the Study of Hypertension in Pregnancy were used to define PE [9]. PE was classified as early (gestational age < 34 weeks at clinical onset) or late ($\geq$34 weeks) [10]. Normotensive healthy women matched for maternal age and gestation were recruited as control subjects from the routine antenatal clinic. A total of 165 pregnancies were finally entered into the study. Approval of the regional ethics committee was obtained, and written informed consent was collected from all of the patients.

Standard 2D and Doppler echocardiographic evaluation, including parasternal and apical views, were performed with subjects in the left lateral decubitus position using a commercially available ultrasound machine and transducer (M5S transducer, Vivid E9; GE Healthcare, Horten, Norway). The following recommended parameters were used by M-Mode in the parasternal long-axis view: interventricular septum (IVSd), posterior wall (PWd), LV end-diastolic (LVd), and end-systolic (LVs) diameters. LV ejection fraction (EF), cardiac output (CO), and stroke volume (SV) were evaluated as previously described [11]. Relative wall thickness (RWT) was calculated as (IVSd + PWd)/LVd. The indices of mitral flow, including the peak early filling (E wave), late diastolic filling (A wave) velocities, deceleration time of E wave (DT), and isovolumic relaxation time (IVRT) were recorded. Tissue pulsed Doppler was recorded in the apical four- and two- chamber view. The average of peak systolic velocities (s'), early diastolic velocities (e'), and late diastolic velocities (a') at the septal, lateral, anterior, and inferior at mitral annulus were computed.

A full-volume scan was acquired by a matrix-array transducer (V4 transducer, Vivid E9; GE Healthcare). From the apical approach, consecutive three-beat electrocardiographically gated subvolume acquisition was performed during apnea to generate the full-volume data set. A 12-slice display mode was selected to ensure the entire LV cavity and walls were included in the full volume (Fig. 1). All data sets were stored digitally in a raw-data format and exported to separate workstations for offline analysis using the 4DAutoLVQ package (EchoPAC PC version 110.1.8, GE Healthcare).

A quad view that displayed the end-diastolic frame was used for manual alignment of the axis and the mitral valve leaflet. Automated border detection and manual correction followed the endocardium throughout the whole cardiac cycle. Next, end-diastolic volume (EDV), end-systolic volume (ESV), SV, CO, EF, and spherical index (SpI) were automatically calculated. Following, to calculate LV mass and myocardial strain, the epicardial border was determined for manual adjustment of the region of interest. After 3D speckle-tracking was utilized in frame-by-frame analysis, the values of regional and global 3D-derived strain were generated and presented as strain curves and a color-coded 17-segment bull's eye plot (Fig. 2). Global longitudinal strain (GLS), global circumferential strain (GCS), global area strain (GAS), and global radial strain (GRS) were calculated as previously reported [12]. The surface of the left atrium was reconstructed and its volume was calculated using a surface algorithm. Maximum and minimum LA volumes were measured using retrospective gating at the end of T wave and at the onset of QRS wave in continuous electrocardiography monitoring. LAEF was defined as the ratio of the difference between the maximum and minimum LA volume to the maximum LA volume.

All image acquisitions were performed at three consecutive beats during breath-holds, and cardiac indices were indexed to body surface area (BSA), following previous study protocols [13].

All imaging data were analyzed by one observer in random order. To test intraobserver variability, a single observer analyzed the data twice on occasions separated by an interval of 1 month. A second observer analyzed the data without knowledge of the measurements of the first observer to test interobserver variability.

Descriptive data are shown as mean $\pm$ SD. Pregnancy data were compared with controls using independent sample *t* tests. Analysis of covariance was used to compare data between EP and LP group. Pearson correlation coefficient was used to analyze the relationship between two parameters. Reproducibility was assessed as the mean percentage error (absolute difference divided by the mean of the 2 observations). We used SPSS version 17.0 (SPSS,

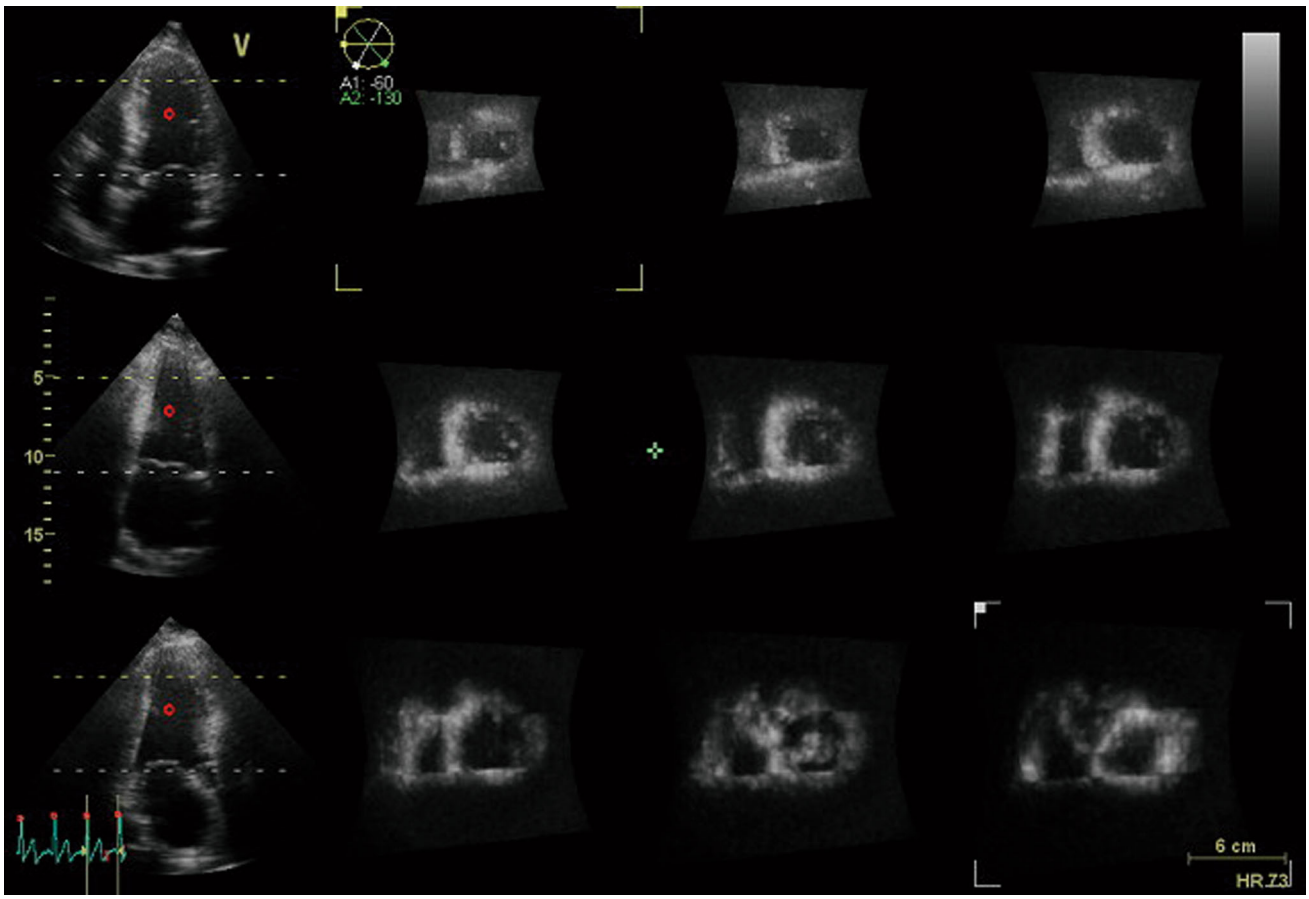

Fig. 1 Twelve-slice display of full-volume mode. Three apical views (four-chamber, two-chamber, and long-axis) and nine short axis views (three basal, three middle, and three apical of the left ventricle). Before storing the volume data set, the operator ensured the entire left ventricular chamber and wall were included in the full volume by 12-slice display mode revealed on the machine

Inc., Chicago, IL) statistical software. $P < 0.05$ was considered to indicate statistical significance.

Results

The clinical and hemodynamic characteristics of the study population are listed in Table 1. These cases were closely matched for age and gestational weeks, respectively. In comparison with controls, both CO indexes declined in women with PE as a result of decreased heart rate. The SV index was reduced by a mean of 9.7 % between EP and LP pregnancy.

Assessment of LV remodeling characteristics is summarized in Table 2. During preeclamptic pregnancy, we observed an enlarged LV chamber and increased RWT versus control subjects; meanwhile, LVMi and SpI were greater in women with PE. In addition, compared with LP, LV volumes and LVMi by 3D STE were obviously greater in EP, and this morphological difference between EP and LP could not be detected by the 2D approach.

Evaluation of LV systolic function is reported in Table 3. The values of FS, tissue Doppler s' and 3D-derived strain indices were remarkably lower in PE women versus normotensive controls. Importantly, a more obvious reduction of GCS, GAS, and GRS was detected in EP women versus LP.

To ensure accuracy, the correlation between 2D and 3D volume assessments is provided in Table 4. There were strong associations in LV volume measurements between 3D and 2D methods.

Table 5 summarizes the changes in LV diastolic function. Compared with control subjects, a declined tissue Doppler e' velocity and significantly an ampliative LA volume index were detected in PE pregnancy. Notably, there was a slight increase in tissue Doppler a' velocity and a mild decrease in the ratio of e'/a' during LP pregnancy, while there was reduced peak A wave velocity and increased ratio of E/e' in EP versus LP.

For LV EDV measurements, intraobserver and interobserver variability were 7.1 and 8.8 %, for 3D EF measurements 6.1 and 7.6 %, for LVMi measurements 9.2 and

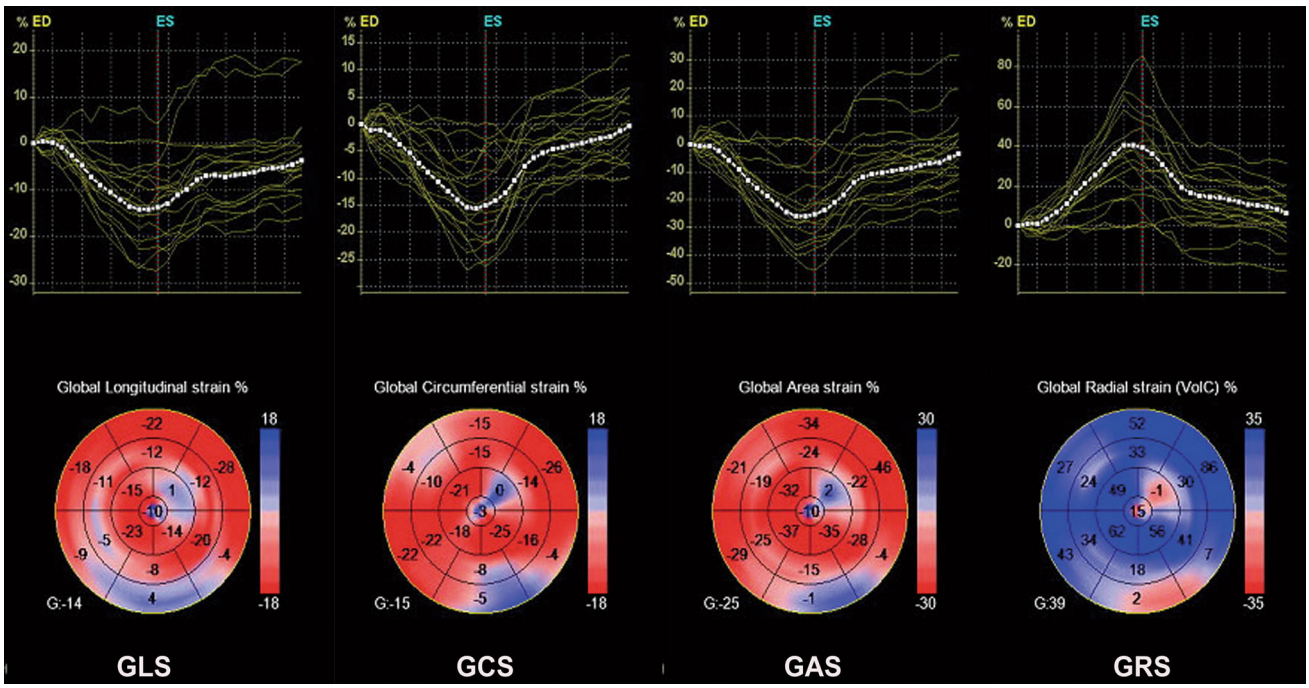

Fig. 2 Strain curves and color-coded 17-segment bull's eye plot. Both strain curves and a color-coded 17-segment bull's eye plot in the preeclamptic women were presented by using the 4DAutoLVQ software package, which in accordance with the values of regional and global directional strains (longitudinal, circumferential, and radial), as well as the area strain. White dotted line indicates global (average) strain, while color lines indicate regional strain. Values of longitudinal strain, circumferential strain, and area strain are negative (*sign* −), whereas values of radial strain are positive (*sign* +). GAS, global area strain; GCS, global circumferential strain; GLS, global longitudinal strain; GRS, global radial strain

Table 1 Clinical and hemodynamic characteristics in normotensive and preeclamptic pregnancy

Variable	Normotensive		Preeclamptic		*P* value		
	N1 (<34w) (n = 41)	N2 (≥34w) (n = 40)	Early (<34w) (n = 43)	Late (≥34w) (n = 41)	N1 versus early	N2 versus late	Early versus late
Age (y)	29.90 ± 5.55	29.03 ± 4.56	32.05 ± 6.42	30.88 ± 5.71	0.106	0.096	0.104
GA (w)	28.20 ± 2.93	36.39 ± 1.29	28.94 ± 2.71	36.43 ± 1.29	0.237	0.898	0.000
GA at delivery (w)	39.40 ± 1.88	39.02 ± 1.14	31.02 ± 3.35	37.23 ± 2.02	0.000	0.001	0.000
BMI (kg/m^2)	24.57 ± 2.26	25.36 ± 1.81	27.91 ± 3.95	29.81 ± 3.20	0.000	0.000	0.318
BSA (m^2)	1.67 ± 0.07	1.71 ± 0.09	1.74 ± 0.15	1.84 ± 0.12	0.006	0.000	0.885
HR (bpm)	89.79 ± 11.89	83.62 ± 13.56	75.25 ± 10.35	80.69 ± 10.95	0.000	0.298	0.228
SBP (mmHg)	104.22 ± 7.62	106.20 ± 8.94	152.81 ± 18.05	143.83 ± 14.23	0.000	0.000	0.000
DBP (mmHg)	67.27 ± 7.07	70.00 ± 7.41	102.44 ± 13.67	98.59 ± 12.79	0.000	0.000	0.367
MBP (mmHg)	79.59 ± 6.39	82.07 ± 7.49	119.23 ± 12.11	113.67 ± 11.61	0.000	0.000	0.297
ci (l min^{-1} m^{-2})	3.43 ± 0.65	3.57 ± 2.40	3.04 ± 0.50	2.96 ± 0.52	0.003	0.029	0.222
svi (ml/m^2)	38.62 ± 5.72	35.45 ± 6.15	40.13 ± 9.09	36.21 ± 8.32	0.367	0.644	0.020
CI (l min^{-1} m^{-2})	3.22 ± 2.82	3.29 ± 0.78	2.21 ± 0.54	2.19 ± 0.40	0.022	0.018	0.065

Data are given as mean ± SD

GA indicates gestational age, *BMI* body mass index, *BSA* body surface area, *HR* heart rate, *SBP* systolic blood pressure, *DBP* diastolic blood pressure, *MBP* mean blood pressure, *ci* cardiac index measured by two-dimensional echocardiography, *svi* stroke volume index two-dimensional echocardiography, *CI* cardiac index measured by three-dimensional echocardiography

Table 2 LV remodeling parameters in normotensive and preeclamptic pregnancy

Variable	Normotensive		Preeclamptic		*P* value		
	N1 (<34w) (n = 41)	N2 (≥34w) (n = 40)	Early (< 34w) (n = 43)	Late (≥34w) (n = 41)	N1 versus early	N2 versus late	Early versus late
2D							
IVSd (mm)	6.84 ± 0.71	6.91 ± 0.73	9.23 ± 1.76	9.04 ± 1.46	0.000	0.000	0.831
LVd (mm)	46.34 ± 3.07	45.63 ± 3.02	49.29 ± 7.42	47.47 ± 4.91	0.020	0.048	0.228
LVs (mm)	30.17 ± 2.48	29.40 ± 2.94	31.69 ± 4.52	31.32 ± 3.70	0.058	0.013	0.762
PWd (mm)	6.87 ± 0.79	7.06 ± 0.60	9.52 ± 1.58	9.21 ± 1.51	0.000	0.000	0.843
RWT	0.30 ± 0.03	0.31 ± 0.03	0.39 ± 0.08	0.39 ± 0.09	0.000	0.000	0.477
3D							
EDV (ml)	83.21 ± 16.35	85.54 ± 17.00	105.16 ± 23.85	98.32 ± 16.70	0.000	0.003	0.002
ESV (ml)	35.18 ± 6.95	37.71 ± 11.45	48.86 ± 17.04	48.00 ± 11.17	0.000	0.001	0.020
EDVi (ml/m^2)	49.89 ± 9.61	49.27 ± 8.65	60.34 ± 11.31	53.80 ± 8.31	0.000	0.035	0.000
LVMi (g/m^2)	62.31 ± 8.70	65.42 ± 7.62	84.09 ± 10.24	75.29 ± 10.13	0.000	0.000	0.012
SpI	0.28 ± 0.04	0.28 ± 0.04	0.38 ± 0.06	0.37 ± 0.10	0.000	0.000	0.910

Data are given as mean ± SD

2D indicates two dimensional echocardiography,*3D* three dimensional echocardiography, *IVSd* interventricular septum diameter,*LVd* left ventricular end-diastolic dimension, *LVs* left ventricular end-systolic dimension, *PWd* posterior wall diameter, *RWT* relative wall thickness, *EDV* left ventricular end-diastolic volume, *ESV* left ventricular end-systolic volume, *EDVi* left ventricular end-diastolic volume index, *LVMi* left ventricular mass index, *SpI* Sphericity index

Table 3 LV systolic function in normotensive and preeclamptic pregnancy

Variable	Normotensive		Preeclamptic		*P* value		
	N1 (<34w) (n = 41)	N2 (≥34w) (n = 40)	Early (<34w) (n = 43)	Late (≥34w) (n = 41)	N1 versus early	N2 versus late	Early versus late
2D							
ef (%)	64.24 ± 3.32	65.08 ± 4.62	62.74 ± 5.54	62.73 ± 4.76	0.139	0.029	0.323
fs (%)	35.54 ± 2.36	36.71 ± 3.75	33.82 ± 3.07	32.10 ± 3.14	0.037	0.017	0.773
s (cm/s)	6.69 ± 1.19	6.84 ± 1.11	4.54 ± 0.85	5.60 ± 1.11	0.000	0.012	0.041
3D							
EF (%)	57.31 ± 4.24	56.25 ± 6.87	54.27 ± 7.69	51.00 ± 7.12	0.039	0.003	0.842
GLS (%)	19.74 ± 2.39	18.28 ± 3.14	15.74 ± 3.19	15.41 ± 2.70	0.000	0.000	0.325
GCS (%)	17.42 ± 2.11	14.97 ± 1.40	15.18 ± 2.76	16.65 ± 3.65	0.022	0.013	0.019
GAS (%)	32.34 ± 3.32	31.19 ± 3.11	26.92 ± 3.67	28.11 ± 3.51	0.000	0.028	0.004
GRS (%)	52.87 ± 8.51	45.75 ± 6.89	40.13 ± 6.98	43.35 ± 6.71	0.000	0.809	0.006

Data are given as mean ± SD

2D indicates two dimensional echocardiography, *3D* three dimensional echocardiography, *EF* ejection fraction, *FS* fractional shortening *s* the average of peak systolic velocities, *GLS* global longitudinal strain, *GCS* global circumferential strain, *GAS* global area strain, *GRS* global radial strain

9.4 %, and for Spl measurements 8.8 and 8.6 %, respectively. Meanwhile, for deformation parameters, intraobserver and interobserver variability were 8.1 and 8.4 % for GLS measurements, 9.4 and 9.2 % for GCS measurements, 7.0 and 8.9 % for GAS measurements, and 9.0 and 11.6 % for GRS measurements, respectively.

Discussion

The present study examined LV structure and function in PE patients by a 3D STE assessment of LV volumes, mass, and strain components. To our knowledge, this is the first study to use the 3D STE approach as an alternative to

Table 4 Univariate relations of left ventricular volumes measured by 3D and 2D echocardiography

Variable	3DE	2DE	*r* coefficient (*P* value)
EDV (ml)	92.83 ± 19.51	101.33 ± 20.82	0.77 (0.008)
ESV (ml)	42.26 ± 8.66	45.84 ± 10.61	0.81 (0.003)
CI (l min^{-1} m^{-2})	2.72 ± 0.84	3.35 ± 1.23	0.71 (0.011)

Data are given as mean ± SD

3DE 3D echocardiography, *2DE* 2D echocardiography, *EDV* end diastolic volume, *ESV* end-systolic volume, *CI* cardiac index

Table 5 LV diastolic function in normotensive and preeclamptic pregnancy

Variable	Normotensive		Preeclamptic		*P* value		
	N1 (<34w) (n = 41)	N2 (≥34w) (n = 40)	Early (< 34w) (n = 43)	Late (≥ 34w) (n = 41)	N1 versus early	N2 versus late	Early versus late
E (m/s)	0.85 ± 0.20	0.84 ± 0.16	0.83 ± 0.21	0.80 ± 0.22	0.671	0.342	0.063
A (m/s)	0.65 ± 0.13	0.68 ± 0.15	0.67 ± 0.14	0.70 ± 0.11	0.567	0.830	0.020
E/A	1.38 ± 0.35	1.26 ± 0.26	1.26 ± 0.43	1.18 ± 0.48	0.090	0.977	0.096
IVRT (ms)	77 ± 19	71 ± 17	74 ± 10	72 ± 9	0.443	0.389	0.201
DT (ms)	186 ± 41	192 ± 34	201 ± 47	188 ± 36	0.348	0.324	0.458
e (cm/s)	9.72 ± 1.53	8.53 ± 1.75	5.67 ± 1.56	5.04 ± 2.16	0.000	0.000	0.509
a (cm/s)	4.70 ± 1.05	5.32 ± 1.25	4.71 ± 1.25	6.33 ± 1.50	0.971	0.081	0.117
e/a	2.02 ± 0.62	1.70 ± 0.55	1.91 ± 1.06	1.20 ± 0.87	0.667	0.080	0.093
E/e	12.46 ± 3.18	13.34 ± 4.33	18.45 ± 5.33	16.78 ± 4.25	0.011	0.027	0.034
LAi (ml/m^2)	22.17 ± 5.29	19.41 ± 5.35	28.42 ± 5.81	30.93 ± 6.00	0.000	0.000	0.317

Data are given as mean ± SD

E indicates peak early diastole transmitral wave velocity, *A* peak late diastole transmitral wave velocity, *IVRT* left ventricular isovolumic relaxation time, *DT* mitral deceleration time, *e* the average of peak early diastolic velocities, *a* the average of peak late diastolic velocities, *LAi* left atrial volume index

standard echocardiography on PE pregnancies and the first report to test the differences in changes of myocardial function between EP and LP. This new approach confirms significant LV remodeling and dramatic changes in the systolic and diastolic function of LV detectable also by standard echocardiography, but allows additional, reliable detection of early myocardial deformation abnormalities and LA remodeling. It is worth noting that global myocardial indices decrease in both EP and LP. In comparison with LP, women with EP experience more exaggerated morphological change, cardiac dysfunction, and myocardial damage.

In this study, PE women exhibited features of eccentric hypertrophy, which are consistent with previous findings obtained by 2DE [14, 15]. LV hypertrophy is an independent predictor of morbidity and mortality [16]. In the current study, patients with EP present a higher LV volume index and a greater LVMi versus LP pregnancies, which indicated a more advanced degree of LV remodeling in EP women. Those changes are likely to be an afterload-mediated LV eccentric remodeling in PE, which are compensatory mechanisms associated with changes in LV from an ellipsoid to a more spherical shape [17]. It is noteworthy that this difference in ventricular remodeling between EP and LP could not be detected by 2D parameters. There was also a substantial difference in the CI measurement between 2D and 3D methods. This is most likely due to, free from any geometric assumption of LV, the volume index and the mass index estimated by 3D STE are more conductive and relatively operator-independent because of its semi-automatic approach [18]. In the current study, the correlation between 2D and 3D volume assessment was good.

The 2DE indices of chamber contractile function in this study, EF and FS, were reduced in women with PE, which was similar to the results of previous studies [19]. However, these parameters are inextricably influenced by the load and the geometry of heart. In this regard, several studies have successfully shown that 3D STE can provide a comprehensive assessment of global and regional LV function through strain analysis in four dimensions [20]. In the present study, 3D-derived LVEF decreased significantly in women with PE, which was in accordance with the results acquired by 2DE. Meanwhile, the values of 3D-derived strain were remarkably reduced in PE patients, which were consistent with the descending of LV chamber

systolic function. According to the force-velocity relation, the increase in blood pressure can decrease myocardial strains, even if LV myocardium is not damaged. Moreover, failure to balance between myocardial oxygen demand and supply, LV will proceed to eccentric hypertrophy accompanied by subendocardial fibrosis detected both in hypertensive subjects and from autopsy data [3, 16]. Therefore, we reasoned that coexistence of LV hypertrophy and reduced 3D-derived strain in PE indicated that there was subendocardial ischemia and/or fibrosis in the myocardial fibers of multiple spatial directions, longitudinal, circumferential, and radial.

Another new and important finding of our study is that, in comparison with LP, lower values of GCS, GAS, and GRS were detected during EP along with similar value of EF. It is likely because of valid contraction band necrosis in PE resulting from coronary artery spasm [3]. Being regarded as different types of the disease [6], EP and LP, therefore, might go through different models of maternal cardiovascular adaptation. Clinical studies show that there is a higher prevalence of asymptomatic dysfunction and higher morbidity and mortality in short- and long-term postpartum cardiovascular impairment during EP rather than LP [21]. Therefore, we deduced there were more remarkable myocardial damages in EP. Notably, GLS in hypertension is reported as the first to be impaired in subclinical LV damage and GCS in hypertensive heart disease is recognized as compensatory mechanism acting to prevent a failure of systolic function in the presence of a subendocardial damage with longitudinal function impairment [22]. However, in our study, there was no significant change in GLS and the value of GCS was higher in LP vs. EP. PE is not just hypertension alone, but a complex complication of pregnancy. Moreover, many different biochemical markers, and genetic and environmental risk factors have been found to be associated with EP and LP [10], which could result in the inconsistency mentioned above.

Interestingly, compared with normal pregnant women, there are no significant changes in value of GRS in LP group. One possible reason is the calculation of GRS depends on both endocardial and epicardial speckle tracking qualities, whereas GLS, GCS, and GAS are estimated only by endocardial data. Thus, GRS measurements might be less accurate and show greater variability. Another reason may be that radial systolic function changes later than longitudinal systolic function in cardiac ischemia [23]. In addition, our data demonstrated that myocardial dysfunction precedes chamber dysfunction and therefore the measurements of 3D-derived strain are able to detect early signs of cardiac abnormality in this hypertensive disorder complicating pregnancy.

The assessment of LV diastolic function should be an integral part of routine examination. According to new diagnoses of heart failure, patients diagnosed with "diastolic heart failing" have normal or nearly normal global EF [24]. In the current study, there was no obvious difference in mitral inflow parameters between normotensive and PE pregnancies. In contrast, a significant decline in tissue Doppler e' velocity and increase in the ratio of E/e' during PE pregnancy strongly illustrated elevation of LV filling pressure in the disease. The amplified LA volume index also reflected the cumulative effects of increased left-sided chamber filling pressures on ventricular and impaired LV relaxation in the disease. Contrary to LP, the lower mitral inflow A wave, the higher ratio of E/e' were detected in EP, which demonstrated raised LV filling pressure, and thus more severely impaired LV relaxation during EP pregnancy.

Limitations and strengths

Although previous studies have shown the cardiovascular implication of PE do not end with the birth of the baby and placenta [13, 18], our study focused on acute cardiac impairment in PE during pregnancy rather than thereafter. Secondly, our study did not include fetal complications and perinatal outcomes. Thirdly, the speckle-tracking analysis highly depended on image quality, which could cause miscorrelation with the low frame rate of 3D STE. Finally, our study only covered a relatively small number of PE women in a single centre, so a large study in the future is required to confirm our results.

The strengths of the present study that were observed included: using 3D STE evaluation, cardiac hypertrophy, and reduced LV function and myocardial dysfunction in PE. Compared with LP, women with EP demonstrated significantly more severe cardiac impairment. These findings have significant clinical implications for better cardiovascular management during PE pregnancy.

Conclusions

Using the 3D STE method, cardiac eccentric hypertrophy, reduced LV systolic and diastolic function, LA remodeling, as well as atrial function abnormalities in PE were observed. Myocardial dysfunction precedes chamber impairment and thus 3D-derived strain measurements may be used for early detection of cardiac disorder in PE. Compared with LP, women with EP demonstrated significantly more severe cardiac impairment. These findings may lead to different strategies of clinical management between EP and LP in the future.

Acknowledgments We thank Songyan Liu and Tianwei Zhao for valuable contributions. This work was supported partially by the Henan Provincial Health research program (Grant ID_201203048) and partially by Henan Province Medical Academic Technology Leaders of Overseas Training Program (Grant ID_201201055).

Conflict of interest None.

References

1. Walker JJ (2000) Pre-eclampsia. Lancet 356:1260–1265
2. Bauer ST, Cleary KL (2009) Cardiopulmonary complications of pre-eclampsia. Semin Perinatol 33:158–165
3. Bauer TW, Moore GW, Hutchins GM (1982) Morphologic evidence for coronary artery spasm in eclampsia. Circulation 65:255–259
4. Hirota Y (1980) A clinical study of left ventricular relaxation. Circulation 62:756–763
5. Yamamoto K, Redfield MM, Nishimura RA (1996) Analysis of left ventricular diastolic function. Heart 75:27–35
6. Von Dadelszen P, Magee LA, Roberts JM (2003) Subclassification of preeclampsia. Hypertens Pregnancy 22:143–148
7. Valensise H, Vasapollo B, Gagliardi G, Novelli GP (2008) Early and late preeclampsia: two different maternal hemodynamic states in the latent phase of the disease. Hypertension 52:873–880
8. Ammar KA, Paterick TE, Khandheria BK, Jan MF, Kramer C, Umland MM, Tercius AJ, Baratta L, Tajik AJ (2012) Myocardial mechanics: understanding and applying three-dimensional speckle tracking echocardiography in clinical practice. Echocardiography 29:861–872 **(Mount Kisco, NY)**
9. Brown MA, Lindheimer MD, de Swiet M, Van Assche A, Moutquin JM (2001) The classification and diagnosis of the hypertensive disorders of pregnancy: statement from the International Society for the Study of Hypertension in Pregnancy (ISSHP). Hypertens Pregnancy 20:IX–XIV
10. Raymond D, Peterson E (2011) A critical review of early-onset and late-onset preeclampsia. Obstet Gynecol Surv 66:497–506
11. Mor-Avi V, Lang RM, Badano LP, Belohlavek M, Cardim NM, Derumeaux G, Galderisi M, Marwick T, Nagueh SF, Sengupta PP, Sicari R, Smiseth OA, Smulevitz B, Takeuchi M, Thomas JD, Vannan M, Voigt JU, Zamorano JL (2011) Current and evolving echocardiographic techniques for the quantitative evaluation of cardiac mechanics: ASE/EAE consensus statement on methodology and indications endorsed by the Japanese Society of Echocardiography. Eur J Echocardiogr 12:167–205
12. Lang RM, Bierig M, Devereux RB, Flachskampf FA, Foster E, Pellikka PA, Picard MH, Roman MJ, Seward J, Shanewise J, Solomon S, Spencer KT, St John Sutton M, Stewart W (2006) Recommendations for chamber quantification. Eur J Echocardiogr 7:79–108
13. Dewey FE, Rosenthal D, Murphy DJ Jr, Froelicher VF, Ashley EA (2008) Does size matter? Clinical applications of scaling cardiac size and function for body size. Circulation 117:2279–2287
14. Simmons LA, Gillin AG, Jeremy RW (2002) Structural and functional changes in left ventricle during normotensive and preeclamptic pregnancy. Am J Physiol Heart Circ Physiol 283:H1627–H1633
15. Melchiorre K, Sutherland GR, Baltabaeva A, Liberati M, Thilaganathan B (2011) Maternal cardiac dysfunction and remodeling in women with preeclampsia at term. Hypertension 57:85–93
16. Huysman JA, Vliegen HW, Van der Laarse A, Eulderink F (1989) Changes in nonmyocyte tissue composition associated with pressure overload of hypertrophic human hearts. Pathol Res Pract 184:577–581
17. Marciniak A, Claus P, Sutherland GR, Marciniak M, Karu T, Baltabaeva A, Merli E, Bijnens B, Jahangiri M (2007) Changes in systolic left ventricular function in isolated mitral regurgitation. A strain rate imaging study. Eur Heart J 28:2627–2636
18. Mor-Avi V, Lang RM (2009) The use of real-time three-dimensional echocardiography for the quantification of left ventricular volumes and function. Curr Opin Cardiol 24:402–409
19. Rafik Hamad R, Larsson A, Pernow J, Bremme K, Eriksson MJ (2009) Assessment of left ventricular structure and function in preeclampsia by echocardiography and cardiovascular biomarkers. J Hypertens 27:2257–2264
20. Kleijn SA, Aly MF, Terwee CB, van Rossum AC, Kamp O (2011) Three-dimensional speckle tracking echocardiography for automatic assessment of global and regional left ventricular function based on area strain. J Am Soc Echocardiogr 24:314–321
21. Melchiorre K, Thilaganathan B (2011) Maternal cardiac function in preeclampsia. Curr Opin Obstet Gynecol 23:440–447
22. Imbalzano E, Zito C, Carerj S, Oreto G, Mandraffino G, Cusma-Piccione M, Di Bella G, Saitta C, Saitta A (2011) Left ventricular function in hypertension: new insight by speckle tracking echocardiography. Echocardiography 28:649–657 **(Mount Kisco, NY)**
23. Bolognesi R, Tsialtas D, Barilli AL, Manca C, Zeppellini R, Javernaro A, Cucchini F (2001) Detection of early abnormalities of left ventricular function by hemodynamic, echo-tissue Doppler imaging, and mitral Doppler flow techniques in patients with coronary artery disease and normal ejection fraction. J Am Soc Echocardiogr 14:764–772
24. Paulus WJ, Tschope C, Sanderson JE, Rusconi C, Flachskampf FA, Rademakers FE, Marino P, Smiseth OA, De Keulenaer G, Leite-Moreira AF, Borbely A, Edes I, Handoko ML, Heymans S, Pezzali N, Pieske B, Dickstein K, Fraser AG, Brutsaert DL (2007) How to diagnose diastolic heart failure: a consensus statement on the diagnosis of heart failure with normal left ventricular ejection fraction by the Heart Failure and Echocardiography Associations of the European Society of Cardiology. Eur Heart J 28:2539–2550